Impact of intelligent control algorithms on demand response flexibility and thermal comfort in a smart grid ready residential building

Fabiano Pallonetto[a], Mattia De Rosa[b,c,*], Donal P. Finn[c]

[a] *School of Business, Maynooth University, Ireland*
[b] *Universitá degli Studi di Sassari, Italy*
[c] *UCD Energy Institute, University College Dublin, Ireland*

Abstract

The present paper investigates the impact of advanced control algorithms on harnessing building energy flexibility in a smart-grid ready full-electric residential building. The impact on thermal comfort is also analysed. The building is located in Ireland and is equipped with a geothermal heat pump and a thermal energy storage system. Two Energy Management systems, based on rule-based and intelligent optimisation algorithm approaches, are developed which use real-time building smart meter and weather data. This data is utilised by various dynamic flexibility metrics within the respective control algorithms. Different time of use tariffs, based on data from the Irish Commission for Energy Regulation and structured on the basis of peak, off-peak and night periods, are also used. Results show that energy cost reductions of up to 21% and 43% can be achieved by the rule-based and intelligent algorithm, respectively, without compromising the thermal comfort within the building. Moreover, total shifting and forcing flexibility potential of up to 34 and 54 kWh, respectively, based on the month of January, can be achieved by the adoption of the intelligent control algorithm.

Keywords: building flexibility, optimisation, control algorithms, smart grids, thermal comfort

*Corresponding author
Email addresses: fabiano.pallonetto@mu.ie (Fabiano Pallonetto), mattia.derosa@ucd.ie (Mattia De Rosa), donal.finn@ucd.ie (Donal P. Finn)

1. Introduction

Increasing global concerns about climate change resulted in the ratification of the Paris agreement under the United Nations Framework Convention on Climate Change (UNFCCC), which aims at maintaining global warming below 2^oC to pre-industrial levels [1]. Following its ratification in 2015, policies dealing with energy consumption and greenhouse gas (GHG) emissions have been enhanced by the European Union by establishing the ambitious targets of 40% carbon emission reduction by 2030 and 60% by 2040, as well as a binding renewable energy target of at least 32% by 2030 [2].

High penetration of Renewable Energy Sources (RES) - such as, wind power integration, solar systems, etc.[3] - together with the electrification of targeted demand categories, are generally recognised as one potential approach to achieve these decarbonisation goals [4]. However, the current power system network, requires a continuous demand/supply balance which can be stressed by the intrinsic volatility of RES production [5]. The conventional sources of flexibility at the generation side may not be sufficient to cope with fluctuations in production generated by RES and, therefore, a paradigm shift towards a coordinated effort between generation, transportation and demand sectors is required [6]. This development - together with the possibility of implementing algorithms to control, schedule and optimise end-use energy consumption and generation - has increased interest in understanding how the potential energy flexibility provided by end-users can be exploited to mitigate the uncertainties associated with high RES penetration in the electricity network [5].

The emerging smart grid framework requires the development of advanced control systems to unlock the deployment of strategies for demand side management (DSM) capable of optimising end-user consumption pattern profiles depending on specific targets and requirements [7–9]. Such a control framework would enable end-users to activate demand response (DR) strategies by which voluntary modification of end use consumption (and generation) patterns can be triggered by direct external requests. For instance, specific tariffs or programs can motivate consumers to respond to changes in the electricity market or to specific network needs, by adjusting their load profile.

The implementation of Demand Response programs have attracted a lot of interest over the last decade due to the benefits at both end-user and power grid network levels. Generally, at the power grid level, DR programs can offer an alternative approach to managing peak load periods to peak power

plants [10]. An optimised power grid network, capable of coping with peak periods through a smart management of the demand side, can enhance its reliability and reduce the capital for infrastructure upgrade otherwise needed, as well as operating costs and, consequently, electricity prices. Moreover, DR programs can lead to a reduction of the overall carbon footprint by unlocking higher penetration of renewable energy generation, both at a district and a centralised grid level, as their intrinsically stochastic production can be mitigated [11]. On the other hand, the smart control system needed to unlock and manage DR programs at an end-use level can lead to more efficient and cost-effective consumption for users. These controls can also enhance the user-adapted thermal comfort and cost control while, at the same time, increase user knowledge and awareness of their own energy consumption [5].

Since the building sector is responsible for about 40% of the overall energy end-use demand worldwide, with the likelihood of additional demand over the coming decades [12, 13], a network of connected buildings capable of activating balancing strategies may represent one potential source of demand flexibility. The implementation of DR programs in buildings requires the deployment of control algorithms capable of optimising building energy load patterns by controlling heating/cooling energy systems to adapt their electricity demand [14]. Such advanced smart control systems can also unlock the exploitation of adaptive thermal comfort [15] and cost optimisation strategies which can lead to a better utilisation of energy resources, while unlocking the building energy flexibility to enable specific services to the grid [11]. Therefore, understanding the energy flexibility potential of building stock has become essential for the implementation and exploitation of DR programs in buildings [16]

Notwithstanding, several challenges and barriers still limit a widespread deployment of DR programs in buildings. One of the major issues is the lack of harmonised, standardised procedures and protocols for assessment of energy flexibility at building level. Specific metrics and quantification tools are required to assess the energy flexibility potential, as well as the cost of DR program implementation and the need for aggregation procedures to scale from individual building to building stock level [17]. Moreover, capturing the dynamic variation of building energy consumption profiles and thermal comfort is essential in order to assess the flexibility potential and to develop efficient control optimisation algorithms for DR programs. Reliable numerical building models, capable of forecasting building energy consumption and comfort status with short time discretisation, must be validated and cali-

brated against metered data in order to detect trade-offs between accuracy and computational cost [18]. However, most control algorithms are developed and trained using only synthetic data, in order to reduce the effort required for calibration and validation as well as negating the need for any associated experimental setup and testing [19].

Generally, the common element in control algorithms is an objective function - which can target financial costs, energy consumption, carbon emissions, etc. - and a set of constraints such as thermal comfort [5]. Typically, rule-based algorithms implement instructions to modify the control set points (i.e., zone temperatures, thermal storage activation, heat pump operation, etc.) as a function of pre-determined boundary conditions. For instance, Yoon et al. [20] developed a rule-based control algorithm aimed at reducing the electricity consumption of a HVAC system as function of the electricity retail price by changing the building internal set-point temperature. Alimohammadisagvand et al. [21] compared four rule-based control algorithms for DR programs in a residential dwelling equipped with a ground-source heat pump and electric resistance heaters. The results showed that savings up to 15% for heating energy consumption can be achieved. Similarly, Salpakari and Lund [22] investigated the shiftable loads available in buildings equipped with PV systems, by using a cost-optimal and rule-based control, which led to a 13-25% cost saving per year. Moreover, the authors demonstrated that coupling PV panels with heat pumps and storage can provide more flexibility potential than other shiftable appliances in residential buildings. On the other hand, the authors also highlighted that further model and controller developments are needed to completely assess the capability of these systems as flexibility sources.

Advanced home energy management systems (EMS), based on the building automation systems, have been shown to be capable of achieving high energy savings and flexibility potential [5]. As illustrated by Paterakis et al. [23], control algorithms embedded in smart thermostats and energy management systems can play a fundamental role to achieve high penetration of renewable energy and to provide a certain level of control of electricity demand. Furthermore, the integration of EMS with the Internet of Things can result in more granular data acquisition and more optimised control at appliance level, while increasing the overall potential demand flexibility and its accurate estimation.

Home Energy Management Systems (EMS) are typically based on reading electricity consumption and other sensors connected to a Home Area Network

(HAN) in order to identify consumption patterns and control of household appliances [24]. However, despite the wide recognition that the performance of DR programs highly depends on the type of control algorithms adopted [21], further research efforts are still needed in order to assess the capabilities of different algorithms in predicting the energy flexibility in households [22]. Compounding this research gap is the need for standardised assessment procedures and protocols which are capable of creating communication channels between the different actors, from building end-users to market stakeholders such as aggregators, the distribution systems operator (DSO) or the transmission system operator (TSO). Ongoing developments in the information and communication technology (ICT) domain may fill this gap in the near future by providing smart tools and algorithms to monitor, assess and aggregate building energy flexibility potential for its exploitation as DR services. However, in the meantime, research efforts need to focus on understanding how to best exploit and control such flexibility sources.

In this context, the present paper investigates the impact of intelligent control algorithms on building energy flexibility potential in a smart grid ready and full-electric residential building. The building is equipped with a photovoltaic system, a ground-source heat pump and a thermal energy storage system. The selected dwelling, described in section 2, is a detached bungalow-type house, located in Ireland and built in the 1970's. Since construction, a progressive retrofitting has been undertaken to meet the current building energy regulations. Two EMS systems were developed based on real-rime smart meter and weather data: a rule-based algorithm and an intelligent control algorithm (section 3). These EMS systems are used to control the building energy consumption/generation pattern in order to identify the energy flexibility potential available for DR programs. The novelty of the algorithm resides not only in the combination of the optimisation technique and the machine learning model used for finding the optimal strategy, but also in using an open source co-simulation framework, which allows decoupling of the building simulation model and the controllers. The performance of the EMS system is compared against specific energy flexibility metrics described in section 4, which allow the assessment of the potential accrued and deferred energy consumption of the analysed building.

2. Experimental test bed

An all-electric residential detached bungalow-type house, representing about 40% of the Irish building stock [25], was selected as a test bed for the assessment of the proposed algorithms. The dwelling consists of a single storey building built in 1973 which was progressively retrofitted in recent years to meet the contemporary standards. The floor area is $205m^2$, and the overall window to wall ratio is 15%, with a 22% and 10% ratio for the south and north facades, respectively [26]. Although the building was built with the typical architectural characteristics in use in the 70s for Irish rural bungalows, its thermal specifications are close to the current Irish building regulation values [27], as reported in Table 1. Moreover, the building thermal performance is aligned with the average Irish residential building, as outlined in the 2020 scenario research published in the Residential Energy Roadmap for Ireland [28], as shown in Pallonetto et al. [29].

Table 1: U-Value of different building elements ([27])

Building Element	**U-Value** (W/m^2K)	
	Test-bed building	*Irish Building Regulations*
Walls	0.25	0.21
Roof	0.25	0.21
Windows	1.7	1.6
Floor	0.21	0.21

The space heating system, illustrated in Figure 1, is a 12 kW (thermal output) ground-source heat pump system coupled with a thermal energy storage tank of 0.8 m^3. Measurements indicated that the secondary working fluid temperature from the ground source field varied typically over a heating season between 8, 6 and 8°C for October, February and May, respectively.

A Heat Recovery Ventilation system was installed. The system extracts heat from the exhaust air to warm incoming fresh air, which is distributed to the bedrooms and living room. The air ducts, located in the attic space, were insulated to reduce thermal losses while the air extraction points were located in the kitchen and bathroom. The particular HRV system has an average sensible heat transfer effectiveness of 80% and operates only during the heating period with a specific fan power of 60W and volume rate of 0.07

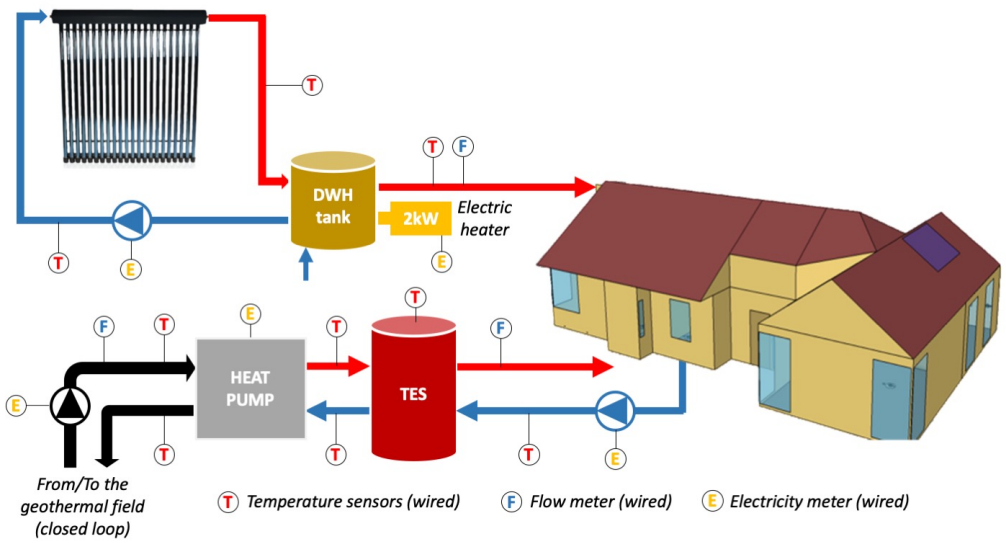

Figure 1: Schematic diagram of the test bed heating system including sensor measurement points.

m^3/s. The air ventilation has been modelled in EnergyPlus exclusively by the operation of the HRV during the heating period, whereas in summer by natural ventilation. During the heating period, for ventilation purposes, the building is divided into two sections with the kitchen/living/bathroom zone considering the cross air mix between the zones and a sleeping/utility zone. The householders' preference was to operate the heat pump during the night time only, in order to take advantage of lower electricity tariffs. Therefore, the heat pump charges the thermal storage during the night-period which is subsequently used during the day time to cover the space heating load. In the context of the current work, this schedule was adopted as the baseline reference.

On the basis of the space heating preferences of the occupants, the heating period was set from the 1st of October to the 30th of April. Table 2 shows the thermostatic set points adopted by the building owner, which are used as hard constraints to develop the control algorithms. These internal set point temperatures refer to the thermostatic controller located in the hallway,

which is the colder part of the building, and they were defined in accordance with the schedule and preference of the occupants. The occupants (i.e., 2 adults) are absent from the house during weekdays between 09:00-16:00 hrs. The process described by Neu et al. [30] was used to replicate the users' activities patterns, which resulted in the distribution of internal heat gains due to their use of appliances, lights and other electric equipment, domestic hot water (DHW), etc.

Table 2: Users' thermostatic set points (^{o}C)

	Weekdays	Weekend
00:00 - 06:30	17 ^{o}C	20 ^{o}C
06:30 - 09:00	19 ^{o}C	20 ^{o}C
09:00 - 16:00	16 ^{o}C	20 ^{o}C
16:00 - 00:00	18 ^{o}C	20 ^{o}C

The building is also equipped with an array of photovoltaic panels with a nominal power of 6 kWp and these are located to the west of house, with a southerly aspect and a 30° inclination. The system has 30 PV panels of 200 Wp each, allocated in three arrays. Moreover, a residential electric vehicle (EV) charging point is installed to supply energy to a Nissan Leaf, with a 24 kWh battery pack. The energy consumption due to charging/discharging cycles of the EV battery is determined considering the EV energy consumption in accordance with Smith [31]. Liaising with the users and analysing historical data of car energy consumption, it was determined that a normalised electricity consumption due to the EV of $150Wh/km$ during the summer and $250Wh/km$ during the winter. Generally, the EV car is plugged in during the evening, but charging starts during the night only to exploit the lower electricity price. The charging pattern suggested by Marra et al. [32] is adopted for the simulations. The selected building was modelled with EnergyPlus [33] followed by calibration of the model using measured data. The calibrated model was subsequently used as a virtual test-bed for development and analysis of flexibility and DR control algorithms. The test bed system uses an open source software called SimApi [34] to send control instructions from the energy management system to the EnergyPlus model during simulation. As illustrated in 2, SimApi and the EMS exchange information through a web based Application Programming Interface (API), while sensor data and control instructions are stored in a database.

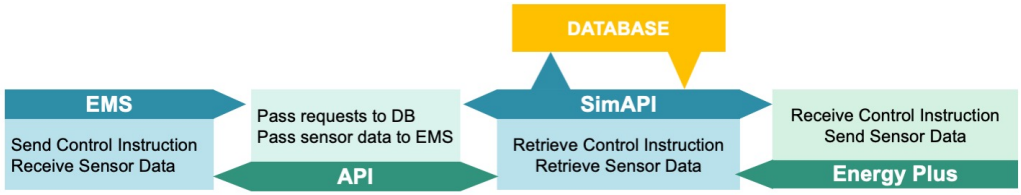

Figure 2: Diagram of the control simulation environment and interaction between the EMS and the building model.

3. Control algorithms

In the current work two EMS with a different control algorithms are compared: a rule-based control algorithm (section 3.1) and an intelligent control algorithm (section 3.3). Both EMS systems use the following objective function, with the aim of minimising the cost associated with household electricity consumption [29]:

$$\min_{T_{tk}, C_{set}, PV_e)} \left[C^T P(T_{tk}, C_{set}, PV_e \right] \tag{1}$$

$$T_{set}(t) - T_{bd} \leq T_{int}(t) \leq T_{set}(t) + T_{bd} \quad t = 1..N \tag{2}$$

$$T_{min} \leq T_{tk} \leq T_{max} \quad t = 1..N \tag{3}$$

where N represents the total timesteps, C is a vector that stores the dynamic electricity price for each timestep in € per kWh, P is the electricity consumption and $P(T_{tk}, C_{set}, PV_e)$ is in kWh, and represents the energy consumption for a timestep t determined by the building simulation model. For the described optimisation problem, three main variables were identified: (i) the storage tank internal temperature (T_{tk}) which ranges between two established set points T_{min} and T_{max}, (ii) the thermal energy supplied to the building zones by means of the circulation pump which can be either enabled or disabled (C_{set}) and, (iii) the energy generated from the renewable energy system, identified as PV_e.

During the simulation, the zone temperature (T_{int}) is maintained at the appropriate set-point (Table 2) and an associated 2^oC bandwidth (i.e., $\pm$ 1^oC around the set point), as shown in Equation 2 and in accordance with Peeters et al. [35] and with the occupants' preference. Moreover, Equation

3 constrains the storage tank temperature between its MIN and MAX temperature settings. The objective function and the constraints reported in Equations 1 to 3 define the solution space for controlling the temperature set point of the storage tank, aiming to minimise the electricity cost, while maintaining indoor thermal comfort.

3.1. Simulation settings and baseline

The assessment of the two EMS systems was performed during a winter month (i.e., January), a period during which peaks of HVAC system usage occur, and this was presented in a previous work [26]. The study was performed by comparing the performance in terms of energy consumption and carbon emissions of the EMS, with a baseline case in which the heating system is controlled by the thermostatic set points only (Table 2), and where no controllers were used to charge or discharge the storage tank. In this condition, the heat pump is switched on whenever needed, even during peak times, to meet the building energy demand. While adopting the same baseline, the present work extends the comparison by analysing the EMS in terms of building thermal comfort and energy flexibility potential by adopting the simulation settings described in section 3.4 and section 4. The details of the rule-based algorithm and the intelligent algorithm are reported in sections 3.1 and 3.3, respectively.

A simulation period of 1 month with 15 minutes resolution was selected to carry out the analysis. The software infrastructure is synchronised to the Building Energy Simulation (BES) model simulation through the database. The API was used to retrieve the data from the co-simulation environment at each time step. Anytime a change in the variable data set occurs, the control system modifies both the heating system and TES thermostatic settings, in accordance with the specific algorithm adopted. If the new updated settings trigger the API controller, the instance status is updated and the mediator waits for the building model to complete the simulation step. This Building Controls Virtual Test Bed (BCVTB), which controls the EnergyPlus instance, sends all sensor results to be stored in the SimApi. Finally, a scheduler collects periodic reports from a monitor and a price predictor component in order to analyse the relevant data and detect an optimal system control schedule to minimise the energy consumption and costs. The management of all household appliances is carried out by the controller, which submits the specific targets and control settings over either a wired or wireless HAN.

Algorithm 1 Rule-based energy management system ([26])

procedure RULE BASED($sensors, time, control$)
  System Initialisation
  Read *sensors*
  Read TCC (thermal comfort constraints)
  if $tc.valid(sensors) = True$ **then** ▷ Check if TCC are satisfied
    if (15:00 $\leq \tau \leq$ 17:00) OR (00:00 $\leq \tau \leq$ 6:00) OR ($PV_{out} \geq 3kW$) **then** ▷ pre-peak or off-peak
      SET the *control* heating system ON to charge TES
    else if 17:00 $\leq \tau \leq$ 19:00 **then**
      SET the *control* heating system OFF
    end if
  else
    SET the *control* heating system ON
  end if
end procedure

The rule-based EMS is based on an algorithm aimed at minimising the energy expenditure (as per Eq. 1) while maintaining building temperature set points as described in Table 2. Four rules are defined to reduce costs and energy consumption by exploiting the thermal energy storage (TES) to shift the energy consumption from high-peak to low-peak tariff periods. The TES charge status is defined by setting the min and max temperatures - i.e., $40°C$ and $60°C$ - according to the system design ([29]). The four rules are described in Algorithm 1.

The control embeds two conditions based on the sensor reading at each time step. The first condition checks if the latest sensor readings have been correctly transmitted and there are no duplicated sensor readings (function *tc.valid*). The second condition checks if the control needs to disable the heating system (typically occurring between 09:00 and 15:00 hrs, when no occupants are in the building). The time step counting variable is incremented only if a valid reading has been detected (condition 1), while the second condition is implemented by switching the circulation pump status and shifting the storage tank set point at its *MIN* temperature. Between 15:00 hrs and 17:00 hrs, the controller enables the heating system, keeping the circulation pump switched off to charge the TES. The control instructions and sensor readings are stored in a database during the whole simulation (a more detailed description can be found in Pallonetto et al. [26]).

3.3. Intelligent control algorithm

The intelligent control algorithm is based on a main operation routing which invokes four main sub-modules. The predictor is based on black box model which implements a machine learning algorithm, which captures the building energy consumption behaviour commencing with historical data, such as internal temperatures, weather data and equipment state [26]. Such a black box modelling approach requires data sensor readings but allows the scalability of the model to different buildings and so replicate the methodology and the algorithms.

The intelligent control algorithm is detailed in Algorithm 2. Firstly, the controller evaluates a violation of the thermostatic set point temperature: if the internal temperature is lower than the thermal comfort set point, the controller will enable the heating system, while skipping a prediction step. If the set point temperature is met, the controller builds a tree of possible solutions performing a status evaluation and a prediction by means of a machine learning model based on a MP5 decision tree. Two datasets were used for training the model and for the prediction of the the internal temperature of the building: (i) a dataset with the GSHP enabled, called $HeatONDB$ and (ii) a dataset with the GSHP turned off, called $HeatOFFDB$. The accuracy of the decision tree model is reported in Table 3. Each tree level represents

Table 3: MP5 decision tree fitting results

	HeatONDB	HeatOFFDB
Pearson Correlation	0.9235	0.7067
MAE	0.0382	0.0724
RMSE	0.122	0.144

a time step prediction which is evaluated against the objective function and thermal comfort constraints. During the tree traversal, the system performs an analysis of the search tree leaves corresponding to the time horizon window. If a tree path state violates the comfort temperature set point, then the algorithm does not build the associated branches from the tree optimising the building time. Each leaf of the tree has an associated energy consumption and cost label and a set of operational instructions for the system. Therefore, the final evaluation of the controller extracts the minimum cost from the search tree data structure.

Additionally, a heuristic function is used for the selection of the storage tank set point temperature (charging or discharging). Given $t_1, .., t_z$ the time

steps in the prediction time horizon, t_0 the current time-step and $P(t_x)$ the electricity price at time-step x, the following function sets the temperature set-point of the storage tank T_{set}:

$$P_k = max(P(t_1), .., P(t_z))$$
$$T_{set} = \begin{cases} T_{max} & \text{if } P_k < 0 \\ T_{min} & \text{if } P_k \geq 0 \end{cases} \quad (4)$$

where T_{max} is the maximum temperature set-point, which is equivalent to a charging mode and T_{min} is the minimum temperature set-point, which is equivalent to a discharging mode.

The function has been built on the basis of the electricity price for the forecast horizon. In an instance where an off-peak price is detected within the forecast horizon, then the storage tank temperature is set to discharging mode so the system can commence exploiting the stored thermal energy. At the end, the algorithm returns the results of the cascade tree of states with updated energy consumption details. Thus, a root child state can provide an the optimal strategy to minimise the energy expenditure and consumption for the next time-step.

Algorithm 2 Intelligent energy management system (Pallonetto et al. [26])

```
procedure INTELLIGENT ALGORITHM(sensors, time, control)
    System Initialisation
    Read sensors
    Read tc thermal comfort constraints
    if tc.valid(sensors) = True then        ▷ Check if thermal comfort constraints are satisfied
        Build a solution tree ts for the time horizon
        Search the leaf_opt = MAX_obj(leaf(tc))
        SET control equal to root(action)-> leaf_opt
    else
        SET the control heating system ON
    end if
end procedure
```

3.4. Time of use tariffs and thermal comfort

The present work extends the comparison by analysing the EMS in terms of building thermal comfort and energy flexibility potential. For this purpose, different Time of Use tariffs, identified in compliance with the Irish

Commission for Energy Regulation ([36]), are analysed. The price scheme (Table 4) is structured on the basis of; *peak*, *off-peak* and *night* tariffs, to reflect the average Irish System Marginal Price (SMP) and consequently of the overall electricity demand.

A thermal comfort evaluation of the baseline, the rule-based and the intelligent algorithm, was carried out for the selected month by using the Fanger Comfort Model [37] integrated within EnergyPlus [38]. This model defines the Predicted Mean Vote (PMV) thermal sensation scale (Table 5) by evaluating the energy exchange mechanisms to a person, coupled with experimentally-derived psychological parameters, to correlate the subjects' response to environmental variables influencing the thermal comfort. Assuming that a person is at steady state with the interior environment, EnergyPlus implements the following correlation to determine the PMV at each time step.

$$PMV = \left(0.303e^{-0.036M} + 0.028\right)(H - L) \tag{5}$$

Terms L, H, M in Equation 5 represent the energy losses from the body (W/m^2), the internal heat production rate of an occupant (W/m^2) and the metabolic rate (W/m^2) respectively, which are calculated as shown in the following equations:

$$L = L_{eva} + L_{resp} + L_{dry} \tag{6}$$

$$H = M - W \tag{7}$$

Being the present case study a residential building, a low-medium metabolic rate ($M = 120W/m^2$) can be assumed in accordance with ISO 8996 [39] and Bröde and Kampmann [40]. The term W (W/m^2) represents the rate of heat loss due to work activities usually ranges from $0 \leq W \leq 0.2M$ [41] and it is difficult to estimate due to the variety of activities which may occur in a residential home. Havenith et al. [41] suggests that for sedentary tasks and tasks with low activity (i.e., standard activities with normal clothing), the value $W = 0$ can be assumed.

4. Energy flexibility and flexibility metrics

The flexibility of a building can be defined as the "*accrued or deferred energy dividend (in kWh) facilitated by thermal storage and residential re-*

Table 4: Time of Use electricity tariffs [€/kWh] ([36].

Hours	**Weekdays**						**Weekends**					
	A	B	C	D	Flat	SMP	A	B	C	D	Flat	SMP
00:00-08:00	0.120	0.110	0.100	0.090	0.135	0.046	0.120	0.110	0.100	0.090	0.135	0.044
08:00-17:00	0.140	0.135	0.130	0.125	0.135	0.065	0.140	0.135	0.130	0.125	0.135	0.062
17:00-19:00	0.200	0.260	0.320	0.380	0.135	0.097	0.140	0.135	0.130	0.125	0.135	0.088
19:00-23:00	0.140	0.135	0.130	0.125	0.135	0.071	0.140	0.135	0.130	0.125	0.135	0.067
23:00-00:00	0.120	0.110	0.100	0.090	0.135	0.053	0.120	0.110	0.100	0.090	0.135	0.053

Table 5: Thermal sensation scale [38]

Sensation	Description
4	Very hot
3	Hot
2	Warm
1	Slightly warm
0	Neutral
-1	Slightly cool
-2	Cool
-3	Cold
-4	Very cold

newable energy generators" [29], enabled by decoupling the building and the energy system. In the case study under analysis, the installed PV system and the TES represent the main source of flexibility, enabled by the possibility of converting the generated electrical energy into thermal energy which, in turn, can be stored in the TES. The state of charge of the TES is represented by its minimum and maximum temperatures, namely 35° and 55°, respectively. In fact, as long as the heat pump control maintains the tank temperature T_{TES} between $T_{TES,max}$ and $T_{TES,min}$, the TES system can be used to meet the heat demand of the building.

Since the system flexibility is directly correlated with the upper and lower temperature bounds of the TES - by means of its thermal capacitance, the heat pump performance and PV production - it is possible to define two parameters measuring the potential of the system to defer energy consumption (i.e., shifting potential S) and/or accrue energy consumption (i.e., forcing potential F). The shifting potential $S(t)$ at the instant t is the sum of the photovoltaic power production PV plus any deferrable heat pump power consumption enabled by the TES system, as shown in Eq. 8. The term SOC_{TES} is State of Charge of the TES, defined as shown in Eq. 9, while COP_{hp} and $Q_{TES,n}$ are the coefficient of performance of the heat pump and the nominal thermal power which can be extracted from the TES when fully charged, respectively.

$$S(t) = \int_{t}^{t+dt} \left(PV(t) + SOC_{TES}(t) \frac{Q_{TES,n}}{COP_{hp}(t)} \right) dt \tag{8}$$

$$SOC_{TES}(t) = \frac{T_{TES}(t) - T_{TES,min}}{T_{TES,max} - T_{TES,min}} \tag{9}$$

Similarly, the forcing potential $F(t)$ is defined as "*the accruable heat pump power consumption when the heat pump thermal output is not used to meet the dwelling thermal demand but is instead stored by the TES system*" [29]. In other words, the heat pump may be forced to operate, even if the internal temperature set point is met, to charge the TES. The maximum amount of electrical energy which can be used to fully charge the TES represents the *flexibility potential* in forcing mode of the system.

$$F(t) = \int_{t}^{t+dt} \left[1 - SOC_{TES}(t)\right] \frac{Q_{TES,n}}{COP_{hp}(t)} dt \tag{10}$$

Both the shifting and forcing potentials can be evaluated at each time step and represent a measure of the energy flexibility available. The next section shows the application of this methodology for the test case described in section 2.

5. Results

An assessment of the energy consumption, carbon emissions and energy costs for the rule-based and intelligent algorithm was undertaken for the 1 month (January) test period.

Figure 3a illustrates the total electricity consumption and carbon emissions due to space heating and DHW production over the 1 month test period. Since the baseline system is controlled by the thermostatic set points only, switching to the more advanced control algorithms leads to a reduction of the building energy consumption by 20.9% and 39% for the rule-based and intelligent algorithms, respectively. This reduction is reflected in the overall carbon emissions (Figure 3a), calculated using 30 minute-averaged historical carbon emissions (gCO_2/kWh), based on technical data from all generation units, including RES, available from the transmission system operator database [42]. Specifically, the footprint ranged from 251 gCO_2/kWh to 643 gCO_2/kWh over the period considered, with maximum values occurring during peak time periods (i.e., 17:00-19:00). Despite the higher percentage of consumption during lower emissions times, the rule-based algorithm shows

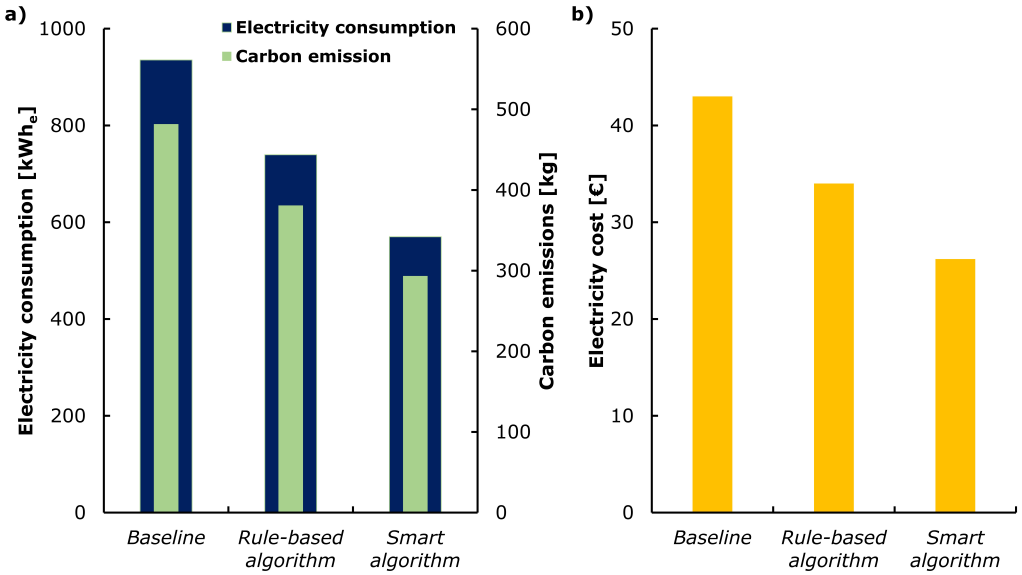

Figure 3: Comparison of control algorithms (1 month test period: January): (a) electricity consumption and carbon emissions, (b) utility electricity production costs.

increased carbon emissions of 20% compared to the intelligent algorithm, due to the less efficient (i.e., non-optimised) control, which led to higher energy consumption. Therefore, carbon intensity becomes a paramount parameter to be included as objective function of control algorithms and/or in the price scheme, in order to lower the building carbon emissions by exploiting the RES penetration at grid level.

Figure 3b shows the generation cost using Irish electricity SMP prices [43] over the period considered. Observing the results from the rule-based algorithm, where the control strategy aims to shift electricity consumption from peak periods (17:00-19:00) to off peak periods (15:00-17:00), a 21% generation cost reduction is observed, while the intelligent algorithm achieves a cost saving up to 43%. Since the difference between the SMP peak and off-peak prices can reach a ratio of up to 6 to 1, which when coupled with the observation that the peaks in the SMP price are aligned with the ToU peak periods, the efficiency of the intelligent algorithm strategy enables the reduction of the total amount of energy consumed by the system and consequently, is capable of leading to utility cost savings.

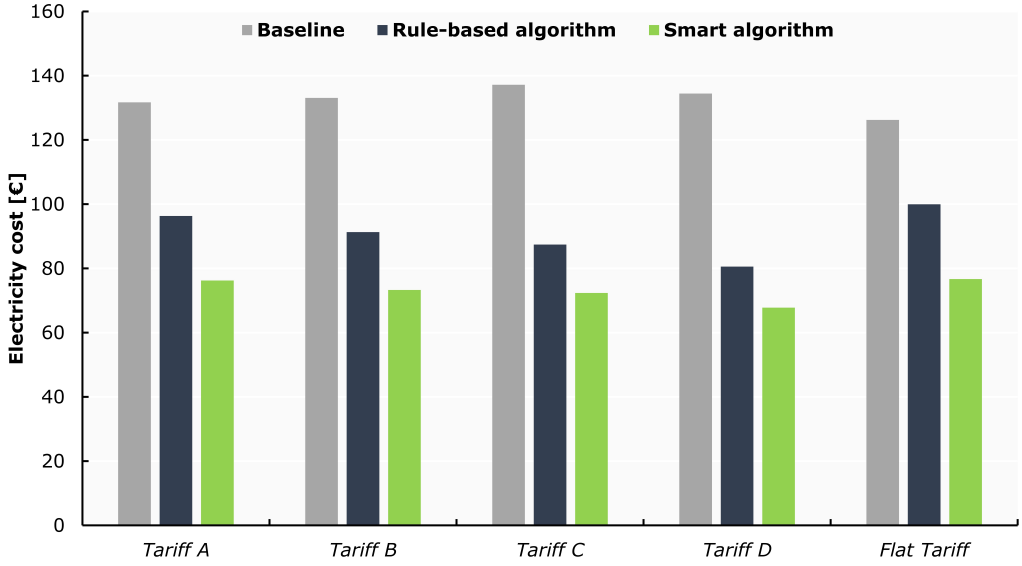

Figure 4: End-use costs for different Time of Use tariffs (Table 4) (1 month test period: January).

In the present work, Time of Use (ToU) tariffs adopted by the Irish smart meter trial [36] are used to assess the consumer electricity cost and to compare the savings obtained by the two different control algorithms described in section 3 and the baseline. Figure 4 shows the electricity cost for the baseline, the rule-based and the intelligent algorithms under different ToU tariffs outlined in Table 4 over the period considered. While the baseline shows the highest cost for all tariffs considered, the rule-based algorithm is capable of providing savings between 27% and 40% depending on the tariff considered (note: Tariff D is the ToU tariff closest to the SMP price). Regarding the intelligent control algorithm, a cost savings between 42% and 49% was achieved. The differences between the rule-based and intelligent algorithms are mainly due to the use of a fixed set of operational rules to control the heating system, which results in a less efficient and, in turn, more expensive charging/discharging schedule of the TES. Finally, the baseline operation of the GSHP during price peaks (17:00 to 19:00) leads to high cost peaks due to the specific price tariff structure, with the result of penalising peak consumption. The adoption of control algorithms (both rule-based and in-

telligent optimisation algorithms) leads to the absence of those peaks, which demonstrate the effectiveness of the algorithms in reducing peak expenditure.

5.1. Thermal comfort assessment

As described in section 3.4, the PMV scoring system is used to assess the thermal comfort of the building based on the equations developed by Fanger and adapted by the ASHRAE [44]. As illustrated in Olesen [45], the ASHRAE standard is compatible to the EN15251 [46]. Therefore, the evaluation of the thermal comfort in the current work adopt the psycho-physical scale shown in Table 5 [47]. Considering also the climatic conditions of the location and the occupants' preferences, thermal discomfort occurs with values outside the range of -1 (slightly cool) to +1 (slightly warm) of the ASHRAE psycho-physical scale.

In order to assess the performance of the controllers in terms of thermal comfort, Figure 5a reports the frequency of the PMV values obtained by the PMV thermal comfort model with a 15 minutes resolution over the period considered. It can be observed that the use of the rule-based and intelligent controller algorithms does not show any thermal comfort violation compared to the baseline. Generally, the intelligent controller provides less thermal comfort variability throughout the day compared to the rule-based controller. However, as evident in the distribution, the intelligent algorithm keeps the inside temperature slightly colder than the baseline.

Further evidence of the thermal comfort performance of the controllers is illustrated in Figure 5b, which reports the average PMV score using box plots for the three algorithms. Despite the small differences in the average PMV scores, the rule-based algorithm exhibits a slightly higher variability and a slightly lower score, while the intelligent algorithm has a similar score compared to the baseline. Concerning the PMV score differences between the three algorithms, the maximum variation is evident between the rule-based and the baseline schemes, and is equivalent to 0.4. The minimum variation between the intelligent algorithm and the rule-based algorithm is 0.03.

Generally, for all control algorithms, the best PMV scores occur during the evening (21:00-22:00) when the occupants are at home and higher internal heat gains increases the overall internal building temperature. It was noted that both algorithms resulted in a similar thermal comfort area, with a moderate negative score evident during the night (01:00-07:00). The rule-based and intelligent algorithm both result in the minimum PMV score (-0.8), which occurs during the day when the temperature set points are lower.

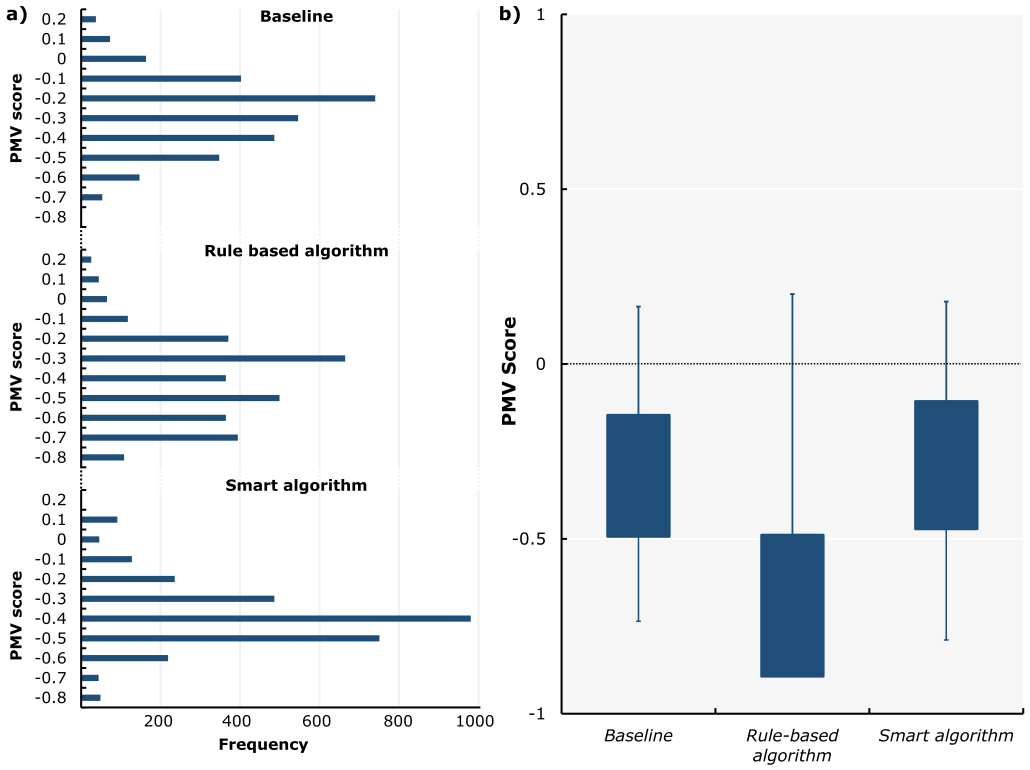

Figure 5: a) Thermal comfort (PMV) frequency histograms and b) Average and standard deviations, for control algorithms (January).

5.2. Flexibility assessment

Considering that the thermal comfort is not affected by the implemented rule-based and intelligent algorithm controllers, as discussed in section 5.1, the analyses was extended to the assessment of the energy flexibility potential by using the metrics described in section 4. In the current work, the main source of flexibility is represented by the TES, assisted by the generation from the renewable source (i.e., PV system). As outlined in section 4, a default lower and upper set point temperatures (i.e, 35^{o}C and 55^{o}C respectively) were chosen with reference to the heat pump nominal thermal output and a system sensitivity analysis. If the tank temperature T_{tk} is maintained between T_{max} and T_{min} by the heat pump, the heat demand of the building can be met by the TES system.

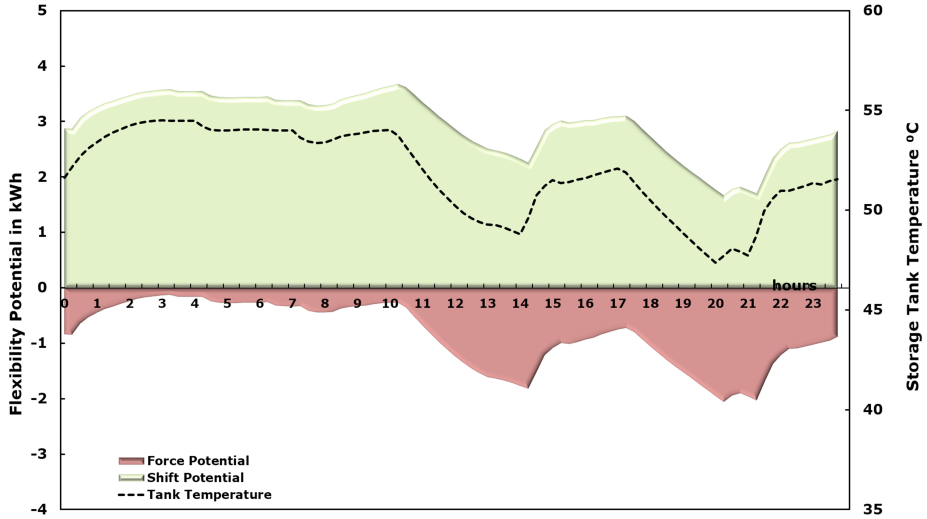

Figure 6: Example of a typical flexibility potential profile for ToU price signal during the winter season.

Figure 6 shows a typical average profile triggered by using a TOU price signal with 2 hours duration. It is noted that if the TES temperature is close to T_{max} (i.e., the TES is fully charged, for an off-peak period), the shifting potential is close to its maximum, whereas the forcing potential reaches its minimum. If heating is required by the building (e.g., between 10:00-14:00) the TES can be discharged, until T_{tk} reaches T_{min}, to cover such demand without active use of the heat pump. This discharging process, reflected by the reduction of the tank temperature, increases the forcing potential or, in other words, the amount of energy which may be stored in the TES for subsequent use. It can be seen from Figure 6 that, after a discharging phase, the TES is charged again just before the beginning of the peak-price period (i.e., between 18:00-20:00 in this example), during which a new discharging phase occurs.

Figure 7 and Figure 8 summarise the cumulative shifting and forcing flexibility of the intelligent algorithm over the test period (i.e., January). Total shifting flexibility potential (Figure 7) is greatest during the weekend and the night, due to the flatter price tariff, while no shifting potential is available during the evening (i.e., negative values) due to the higher energy demand required by the building, as well as the higher tariffs. On the other hand, the forcing flexibility potential (Figure 8) is typically greater for weekdays,

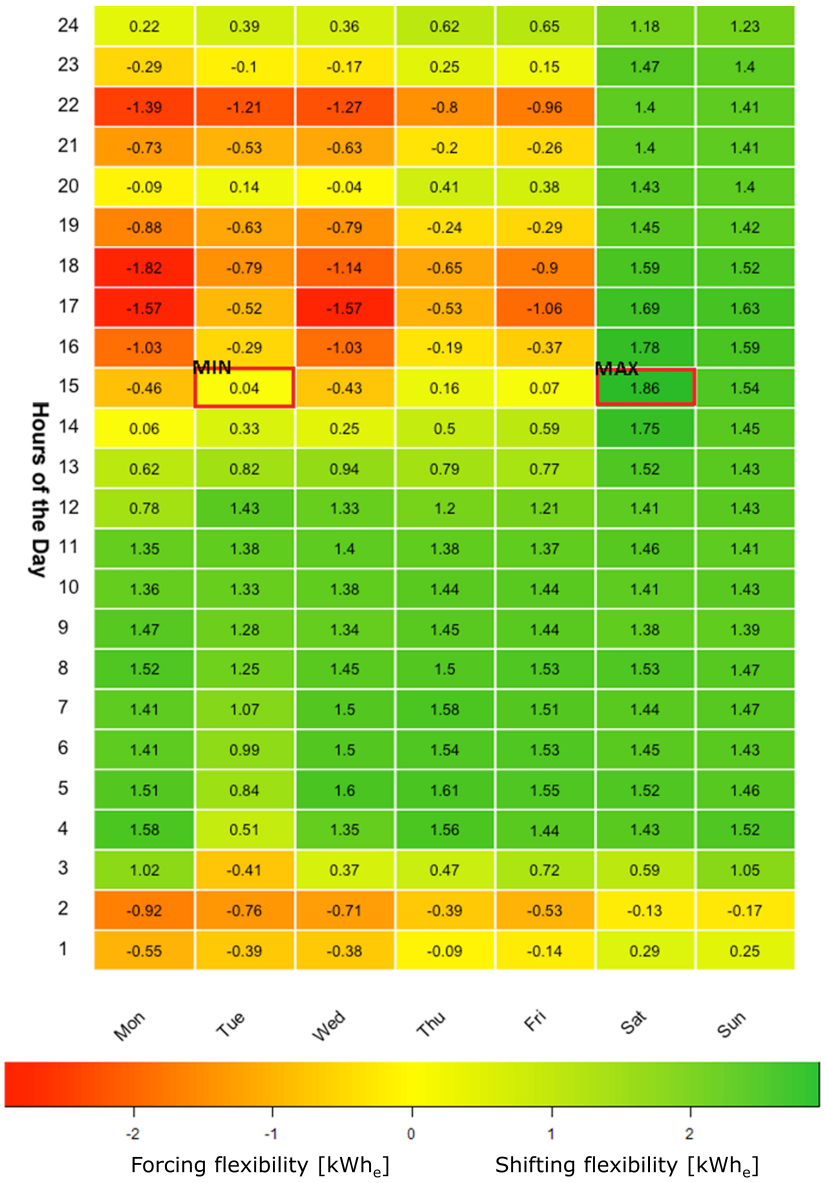

Figure 7: Average hourly shifting flexibility (S) obtained with the intelligent algorithm under Tariff D (in kWh_e) (1 month test period: January).

due to the higher building temperature set point and the flat tariff. It can be seen that higher forcing potentials occur during the late evening and night (i.e., 10 pm - 3 am), since the heat pump can be forced to charge the TES

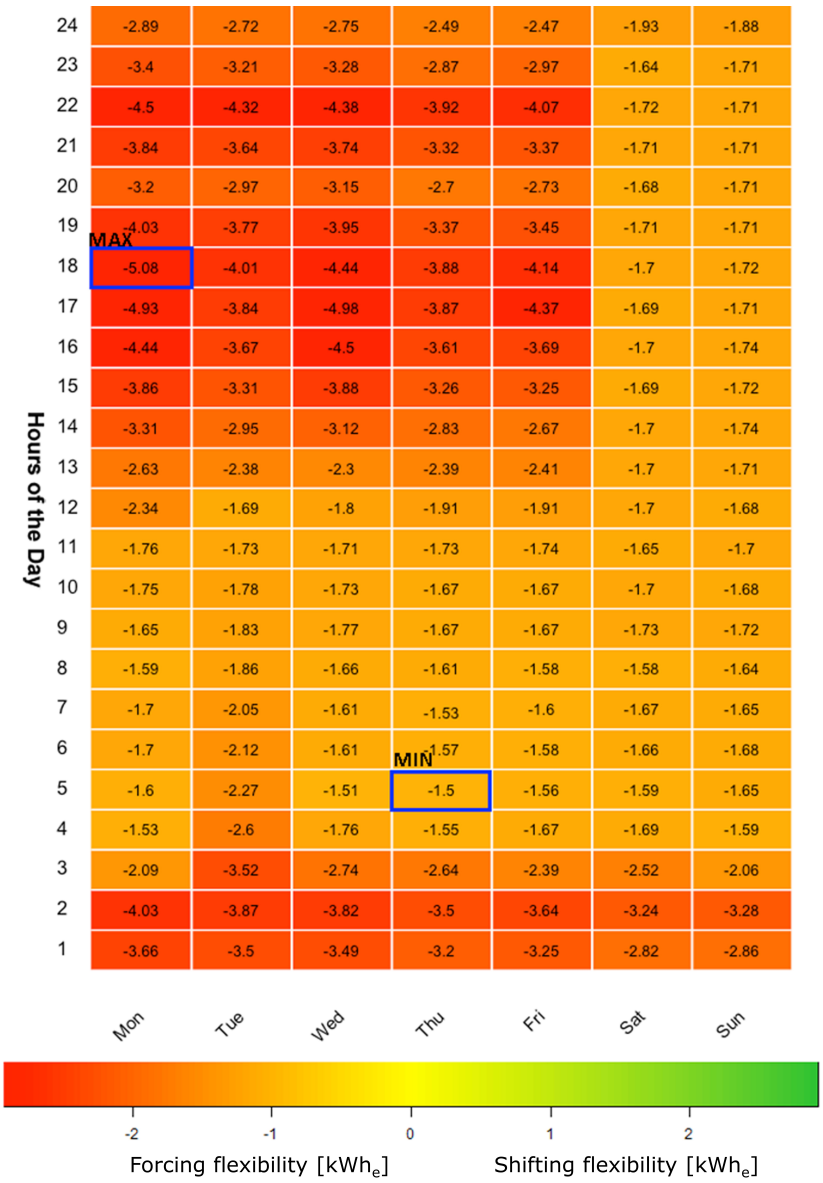

Figure 8: Average hourly forcing flexibility (F) for the intelligent algorithm under Tariff D (kWh_e per day) (1 month test period: January).

by exploiting the lower tariffs. As the TES is charged, the forcing potential reaches its minimum, corresponding to the energy demand required to keep the TES at its maximum temperature. Moreover, greater values of the forc-

ing potential can be observed to occur in the late afternoon and evening (i.e., 2 pm - 10 pm), since the TES is typically discharged to cover the building demand due to the peak tariff period. This period corresponds to the absence of shifting potential observed in Figure 7, as explained earlier.

Figure 9 reports the hourly average flexibility obtained by the different controllers for the 24 hour period considered, as per Figure 6. As illustrated in Figure 9 (a,b), the rule-based and the baseline results exhibit a negative bias toward forcing flexibility. The baseline shows the highest imbalance between the two flexibility components. While the baseline system under utilises the TES, keeping it always almost fully charged, the intelligent algorithms has a negative bias toward the shifting flexibility. Such a bias could affect the thermal comfort of the building in the scenario of extremely cold weather.

The baseline forcing flexibility is equivalent to 7.86 kWh (0.25 kWh per day) while shifting flexibility is equal to 81.49 kWh (2.62 kWh per day) over the considered period (i.e., January). The rule-based cumulative hourly flexibility for the shifting potential is equivalent it 64.13 kWh (2.0 kWh per day), while the forcing potential is 25.22 kWh (0.81 kWh per day). The accumulated total daily flexibility potential for the intelligent algorithm over the testing period, shows a total shifting and forcing potential of 34.52 kWh and 54.82 kWh, respectively, which if averaged on a daily basis is approximately 1.1 kWh and 1.76 kWh per day.

6. Conclusions

The present paper investigated the impact of the use of advanced control algorithms on building energy flexibility potential and thermal comfort in a smart grid ready and full-electric residential building equipped with a geothermal heat pump and thermal storage. With reference to the specific case study analysed in the present paper, the adoption of more advanced control algorithms leads to a promising reduction of the building energy consumption of 20.9% and 39% for the rule-based and intelligent algorithm, respectively. Moreover, switching the electricity consumption from peak to off-peak periods leads to a 21% cost reduction if the rule-based control is adopted, while the intelligent algorithm can achieve cost reductions of up to 43% compared to the baseline, where no optimisation controls are implemented. Since the rule-based algorithms adopts a fixed set of operational rules to control the heating system, a less efficient and, in turn, more expensive charging/discharging schedule of the TES occurs. This leads to the

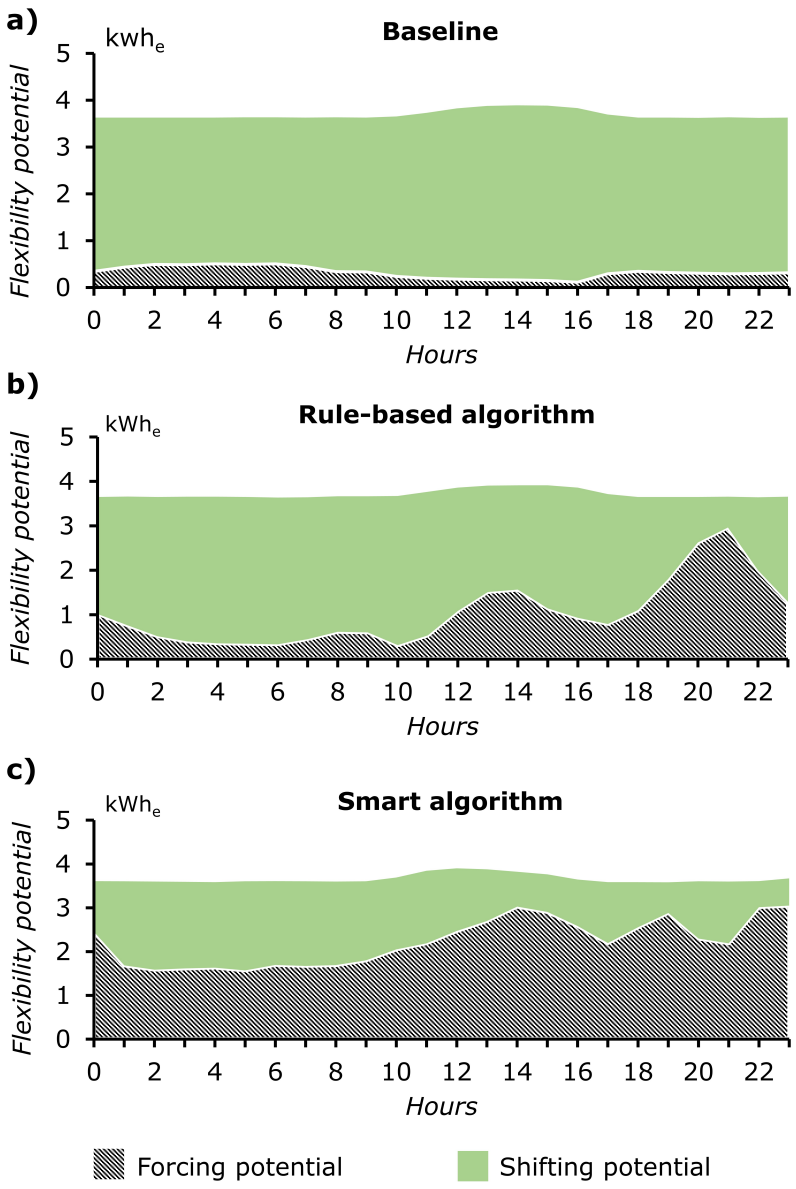

Figure 9: Average forcing and shifting potential over the testing period) (1 month test period: January): (a) baseline, (b) rule-based and (c) intelligent algorithm.

differences of the results obtained from the rule-based and intelligent optimisation algorithms. Both the control algorithms analysed showed similar thermal comfort levels, with no violation of the PMV limit and only moderate

negative values during night periods (minimum PMV value of -0.8 PMV).

From a flexibility perspective, the intelligent algorithm operates the TES closer to the lower temperature set point to reduce overall energy consumption and costs. Consequently, the shifting flexibility compared to the forcing flexibility is lower. Total shifting potential is greatest during weekend and night periods due to flatter price tariffs, while there is little or no availability during the evening due to the high building demand. The forcing potential is typically greater for weekdays due to the higher building temperature set point and the flat tariff.

Moreover, it is noted that the flexibility metrics adopted in the present work (section 4) outlining the capability of the system to defer or accrue the energy consumption depending on specific external variables (i.e., ToU tariffs), meets the energy needs and thermal comfort constraints of the residential building. The extracted information may be useful for aggregators to assess and aggregate the total potential flexibility of a residential building stock. Further research is however required to develop a comprehensive method for profile and metrics aggregation.

Finally, it is important to state that, while the results described in the present work are case-specific and refer to the particular application described in section 2, the methodology adopted - i.e., the control algorithms (section 3) and the flexibility metrics (section 4) have the potential to be readily adapted and used in other building energy applications.

Acknowledgements

This work was conducted in the Electricity Research Centre, University College Dublin, Ireland, which is supported by the Commission for Energy Regulation, Bord Gais Energy, Bord na Mona Energy, Cylon Controls, EirGrid, Electric Ireland, ESIPP, Energia, EPRI, ESB International, ESB Networks, Gaelectric, Intel, SSE Renewables and UTRC. This publication has emanated from research conducted with the financial support of PRLTI[R12681]. The authors would like to thank the building owners for their essential support.

References

[1] J. Rogelj, M. Den Elzen, N. Höhne, T. Fransen, H. Fekete, H. Winkler, R. Schaeffer, F. Sha, K. Riahi, M. Meinshausen, Paris Agreement cli-

mate proposals need a boost to keep warming well below 2^oC, Nature 534 (2016) 631–639.

[2] European Union, 2050 Climate & Energy package, `https://ec.europa.eu/clima/policies/strategies/2050_en`, 2017. 2017-04-03.

[3] K. Hedegaard, B. V. Mathiesen, H. Lund, P. Heiselberg, Wind power integration using individual heat pumps–analysis of different heat storage options, Energy 47 (2012) 284–293.

[4] R. El Geneidy, B. Howard, Contracted energy flexibility characteristics of communities: Analysis of a control strategy for demand response, Applied Energy 263 (2020) 114600.

[5] F. Pallonetto, M. De Rosa, F. D'Ettorre, D. P. Finn, On the assessment and control optimisation of demand response programs in residential buildings, Renewable and Sustainable Energy Reviews 127 (2020) 109861.

[6] H. Lund, A. N. Andersen, P. A. Østergaard, B. V. Mathiesen, D. Connolly, From electricity smart grids to smart energy systems–a market operation based approach and understanding, Energy 42 (2012) 96–102.

[7] L. Gelazanskas, K. A. Gamage, Demand side management in smart grid: A review and proposals for future direction, Sustainable Cities and Society 11 (2014) 22 – 30.

[8] A. Kathirgamanathan, M. De Rosa, E. Mangina, D. P. Finn, Data-driven predictive control for unlocking building energy flexibility: A review, Renewable and Sustainable Energy Reviews 135 (2020) 110120.

[9] B. V. Mathiesen, H. Lund, D. Connolly, H. Wenzel, P. A. Østergaard, B. Möller, S. Nielsen, I. Ridjan, P. Karnøe, K. Sperling, et al., Smart energy systems for coherent 100% renewable energy and transport solutions, Applied Energy 145 (2015) 139–154.

[10] M. Aghamohamadi, M. E. Hajiabadi, M. Samadi, A novel approach to multi energy system operation in response to dr programs; an application to incentive-based and time-based schemes, Energy 156 (2018) 534 – 547.

[11] P. Fitzpatrick, F. DEttorre, M. De Rosa, M. Yadack, U. Eicker, D. P. Finn, Influence of electricity prices on energy flexibility of integrated hybrid heat pump and thermal storage systems in a residential building, Energy and Buildings (2020) 110142.

[12] D. Drysdale, B. V. Mathiesen, S. Paardekooper, Transitioning to a 100% renewable energy system in denmark by 2050: Assessing the impact from expanding the building stock at the same time, Energy Efficiency 12 (2019) 37–55.

[13] M. Carragher, M. De Rosa, A. Kathirgamanathan, D. P. Finn, Investment analysis of gas-turbine combined heat and power systems for commercial buildings under different climatic and market scenarios, Energy Conversion and Management 183 (2019) 35 – 49.

[14] B. Alimohammadisagvand, J. Jokisalo, S. Kilpeläinen, M. Ali, K. Sirén, Cost-optimal thermal energy storage system for a residential building with heat pump heating and demand response control, Applied Energy 174 (2016) 275–287.

[15] J. F. Nicol, M. A. Humphreys, Adaptive thermal comfort and sustainable thermal standards for buildings, Energy and buildings 34 (2002) 563–572.

[16] A. Kathirgamanathan, T. Péan, K. Zhang, M. De Rosa, J. Salom, M. Kummert, D. P. Finn, Towards standardising market-independent indicators for quantifying energy flexibility in buildings, Energy and Buildings (2020) 110027.

[17] L. Zhang, N. Good, P. Mancarella, Building-to-grid flexibility: Modelling and assessment metrics for residential demand response from heat pump aggregations, Applied Energy 233 (2019) 709–723.

[18] M. De Rosa, M. Brennenstuhl, C. Andrade Cabrera, U. Eicker, D. P. Finn, An iterative methodology for model complexity reduction in residential building simulation, Energies 12 (2019) 2448.

[19] R. Lu, S. H. Hong, Incentive-based demand response for smart grid with reinforcement learning and deep neural network, Applied Energy 236 (2019) 937 – 949.

[20] J. H. Yoon, R. Baldick, A. Novoselac, Dynamic demand response controller based on real-time retail price for residential buildings, IEEE Transactions on Smart Grid 5 (2014) 121–129.

[21] B. Alimohammadisagvand, J. Jokisalo, K. Sirén, Comparison of four rule-based demand response control algorithms in an electrically and heat pump-heated residential building, Applied Energy 209 (2018) 167–179.

[22] J. Salpakari, P. Lund, Optimal and rule-based control strategies for energy flexibility in buildings with pv, Applied Energy 161 (2016) 425–436.

[23] N. G. Paterakis, O. Erdin, J. P. Catalo, An overview of demand response: Key-elements and international experience, Renewable and Sustainable Energy Reviews 69 (2017) 871–891.

[24] D. Ren, H. Li, Y. Ji, Home energy management system for the residential load control based on the price prediction, in: Online Conference on Green Communications (GreenCom), 2011 IEEE, pp. 1–6.

[25] Ireland Central Statistics Office, The roof over our heads, `http://www.cso.ie`, 2012.

[26] F. Pallonetto, M. De Rosa, F. Milano, D. P. Finn, Demand response algorithms for smart-grid ready residential buildings using machine learning models, Applied Energy 239 (2019) 1265 – 1282.

[27] Irish Building Regulations, Building regulations 2011, conservation of fuel and energy - dwellings, 2011.

[28] SEAI, Residential energy road map, Online, 2011.

[29] F. Pallonetto, S. Oxizidis, F. Milano, D. Finn, The effect of time-of-use tariffs on the demand response flexibility of an all-electric smart-grid-ready dwelling, Energy and Buildings 128 (2016) 56 – 67.

[30] O. Neu, S. Oxidis, D. Flynn, F. Pallonetto, D. Finn, High resolution space-time data: methodology for residential building simulation modelling, IPBSA (2013).

[31] W. J. Smith, Can ev (electric vehicles) address ireland carbon emissions from transport?, Energy 35 (2010) 4514–4521.

[32] F. Marra, G. Y. Yang, C. Træholt, E. Larsen, C. N. Rasmussen, S. You, Demand profile study of battery electric vehicle under different charging options, in: 2012 IEEE Power and Energy Society General Meeting, pp. 1–7.

[33] D. B. Crawley, L. K. Lawrie, F. C. Winkelmann, W. F. Buhl, Y. J. Huang, C. O. Pedersen, R. K. Strand, R. J. Liesen, D. E. Fisher, M. J. Witte, et al., Energyplus: creating a new-generation building energy simulation program, Energy and buildings 33 (2001) 319–331.

[34] F. Pallonetto, E. Mangina, F. Milano, D. P. Finn, Simapi, a smart-grid co-simulation software platform for benchmarking building control algorithms, SoftwareX 9 (2019) 271 – 281.

[35] L. Peeters, R. De Dear, J. Hensen, W. Dhaeseleer, Thermal comfort in residential buildings: Comfort values and scales for building energy simulation, Applied energy 86 (2009) 772–780.

[36] CER, Smart metering cost-benefit analysis and trials findings reports., 2012.

[37] P. O. Fanger, et al., Thermal comfort. analysis and applications in environmental engineering., Thermal comfort. Analysis and applications in environmental engineering. (1970).

[38] US Department of Energy, Energy Plus Version 9.4.0 Documentation, `https://energyplus.net/sites/all/modules/custom/nrel_custom/pdfs/pdfs_v9.4.0/EngineeringReference.pdf`, 2020. 2020-09-29.

[39] International Organisation for Standardisation, Ergonomics of the thermal environment - Determination of metabolic rate, `https://www.iso.org/standard/34251.html`, 2004.

[40] P. Bröde, B. Kampmann, Accuracy of metabolic rate estimates from heart rate under heat stressan empirical validation study concerning iso 8996, Industrial health (2018).

[41] G. Havenith, I. Holmér, K. Parsons, Personal factors in thermal comfort assessment: clothing properties and metabolic heat production, Energy and buildings 34 (2002) 581–591.

[42] J. Torriti, M. G. Hassan, M. Leach, Demand response experience in europe: Policies, programmes and implementation, Energy 35 (2010) 1575–1583.

[43] Semo, Single electricity market operator, 2015.

[44] ASHRAE, Ashrae standard 55 - thermal environmental conditions for human occupancy, 2017.

[45] B. W. Olesen, The philosophy behind en15251: Indoor environmental criteria for design and calculation of energy performance of buildings, Energy and Buildings 39 (2007) 740–749. Comfort and Energy Use in Buildings - Getting Them Right.

[46] EN 15251, Indoor environmental input parameters for design and assessment of energy performance of buildings- addressing indoor air quality, thermal environment, lighting and acoustics, 2007.

[47] L. Peeters, R. de Dear, J. Hensen, W. Dhaeseleer, Thermal comfort in residential buildings: Comfort values and scales for building energy simulation, Applied Energy 86 (2009) 77–80.